Full Length Article

Corrosion and wettability of PEO coatings on magnesium by addition of potassium stearate

S.S. Farhadi, M. Aliofkhazraei *, Gh. Barati Darband, A. Abolhasani, A. Sabour Rouhaghdam

Department of Materials Science, Faculty of Engineering, Tarbiat Modares University, P.O.Box: 14115-143, Tehran, Iran

Abstract

Hydrophobic PEO coatings were fabricated in an electrolyte containing potassium stearate. The wetting behaviour of coated samples was studied using dynamic and static contact angle. Also, the corrosion behaviour of the samples was evaluated by polarization method. The dynamic contact angle and hysteresis of the contact angle for PEO coating were evaluated by Wilhelmy plate method. There was an increase in the contact angle of the nanocomposite and traditional PEO coatings when potassium stearate was added to the electrolyte up to 130°. The more hydrophobic coatings, showed more corrosion resistance in 3.5 wt.% NaCl solution. The synergistic effect of potassium stearate and nanoparticles increased the hydrophobicity because of assembling of fatty acid on ceramic powder.

1. Introduction

Plasma electrolytic oxidation (PEO), also known as Micro Arc Oxidation (MAO), is a promising novel process which has the capacity of fabricating a stable and adherent oxide layer on metals, such as Mg. This process is based on the anodic oxidation of the metal when connected to the high-voltage source which has been immersed in a proper electrolyte. The combination of the electrolyte solution has an effect on the stability of the passive layer, size and distribution of sparks and formed phases.

PEO process provides the possibility for fabrication of hydrophobic coatings. The method of PEO on magnesium (Mg), by incorporation of PTFE nanoparticles suspended in electrolyte in a single step, were used for the fabrication of a thick and hydrophobic coating layer [1]. These PTFE containing coatings shift the corrosion potential to more noble values and consequently, decrease the corrosion rate [1]. In some papers, saturated fatty acids have also been used in two steps after oxidizing [2]. Anodized aluminium was used as a substrate for treatment with dilute ethanolic solution of stearic acid, and super hydrophobic coating

was fabricated [3]. Myristic fatty acid in the form of ethanolic solution and pure molten acid also have been used to modify the surface energy of anodized aluminium coatings [4].

PEO can also serve as a pre-process for another coating process in order to attain any arbitrary wetting contact angle for coating. Multiple-step superhydrophobic coating on the surface of magnesium has been investigated by researchers [5,6], using PEO treatment. Sol-gel method has been applied for the deposition of silane compounds on magnesium substrate [7]. PEO coating is much more noble than nanocomposite silane. Therefore, the coating formed by adding silane to pure PEO becomes generally more active; however, due to superhydrophobicity, its corrosion resistance increases [7].

In this paper, one-step method was used for the fabrication of a hydrophobic PEO coating. Saturated fatty acids containing hydroxyl groups were added to the electrolyte of PEO in order to react with the surface and to make it hydrophobic on Mg substrate. Presence of nano and micro roughness are necessary for superhydrophobic coating [8] and nanoroughness can be gained by nanoparticle. In this paper, silicon nitride nanoparticles were added to coating electrolyte to attain nanoroughness on surface.

The Wilhelmy plate technique is one of the most accurate methods for measuring dynamic contact angles, and it is superior to the other methods [9] due to the following reasons: (1) precision of contact angle estimation due to detection with

* Corresponding author. Department of Materials Science, Faculty of Engineering, Tarbiat Modares University, P.O. Box: 14115-143, Tehran, Iran.
E-mail addresses: maliofkh@gmail.com, khazraei@modares.ac.ir (M. Aliofkhazraei).

a sensitive microbalance, which is free from the operator error arising from determination by eye; (2) high reproducibility due to the large scanning area of substrates (centimetres across) and bulk liquid.

2. Experimental

Investigated variables in this paper are the concentration of the potassium stearate in the presence and absence of nanoparticle. In this study, commercially pure magnesium alloy sheet having a thickness of 1 mm was utilized. Samples were prepared in square shapes with equal sides of 3 cm. Before PEO coating process, acid pickling process was carried out in 10 wt.% sulfuric acid solution. A home-made 20 kW PEO coating system with stainless steel cathode was used. A neutralization process of potassium hydroxide of pure stearic acid was chosen to generate potassium stearate ($C_{18}H_{35}KO_2$). Then potassium stearate was dissolved in electrolyte of PEO coating at 80 °C. Besides, silicon nitride nanoparticle was used as suspension inside the electrolyte. The TEM image of used silicon nitride (Si_3N_4 − average size of 37 nm) nanoparticle was captured using a Philips CM-180 transmission electron microscope (Fig. 1). Pure sodium phosphate with a concentration of 8 g/L served as the base of the electrolyte. Potential variations during the coating process were registered using a professional APPA 505 multimeter, with a sample rate of 2 samples per second. PEO coating process was performed by determining two additive concentrations in the presence and absence of Si_3N_4 (Table 1). The time taken for the coating process and its current density were 5 min and 28 mA/cm², respectively.
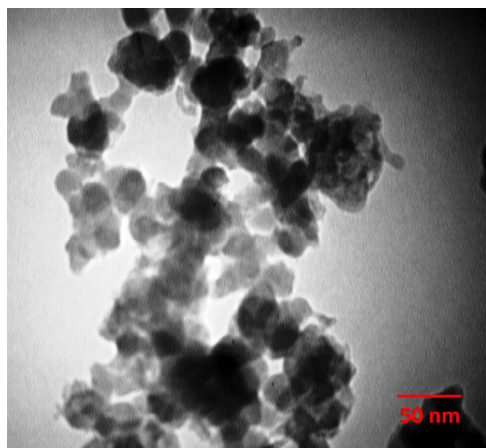
During the roughness test, the average roughness (R_a) of all coatings was measured using the Taylor Hobson Surtronic-25 roughness tester. To investigate the surface morphology of the samples, a Philips XL30 scanning electron microscope (SEM) was used. The TEM of samples was captured using a Zeiss − EM10C − 80 KV TEM.

To evaluate the wettability of coatings, two concepts including static and dynamic contact angle and contact angle hysteresis should be considered. The study of wetting under dynamic conditions can be performed using the Wilhelmy plate method, by recording the force acting on the solid as it moves through the liquid/air interface at a constant speed.

The AND GR-202 analytical balance was coupled to a hydro-pump for conduction of the Wilhelmy plate test. The test was carried out at an immersion rate of 0.15 mm/s. Measurement of contact angle was done using the AM413zt Dino-lite digital microscope. 10 µL drops of deionized water were infused on the specimen surface. An image analyzer was used to measure the arc length facing the intersection of drop–surface interaction which is equal to the sum of the two interior angles. An average of 6 contact angle measurements was used as the results of the static contact angle.

Electrochemical tests were carried out via polarization performed by the EG&G model 273A potentiostat/galvanostat in 3.5 wt.% NaCl solution. After half an hour, when all of the coatings have reached their stable open circuit potentials (OCP), test was carried out in a flat cell of 0.21 cm² area. Then, polarization test was performed between −0.3V and +0.3V versus OCP. Corrosion test was done using power suite version 2.5 software with scan rate and scan height of 1 and 2 mV/s, respectively. The calomel reference electrode was used.

3. Results and discussion

The coating roughness of different samples is presented in Table 2. The roughness results for S-0-1 and R-0-0 samples show that the additive caused a great increase in roughness criterion to 1.89 µm. A comparison of S-0-1 and S-0-2 samples revealed that the concentration of potassium stearate is inversely correlated with the roughness, and also R_a reached 1.6 µm. Effects of potassium stearate on roughness of nanocomposite coating are similar to the behaviour of traditional coatings in the presence of additive. It seems that the nanoparticle suspension decreased in surface roughness and this value is in good agreement with the results of other researchers [10].

Fig. 2 illustrates the SEM images of different samples. High magnification on the nanocomposite coatings (Fig. 3) revealed

Fig. 1. TEM image of Si_3N_4 nanopowder.

Table 1
Combination and condition of coating process.

Sample code	Nano powder concentrate (g/L)	Additive concentrate (g/L)
S-0-1	0	1
S-0-2	0	2
S-5-1	5	1
S-5-2	5	2
R-0-0	0	0
R-5-0	5	0

Table 2
Roughness of the coatings.

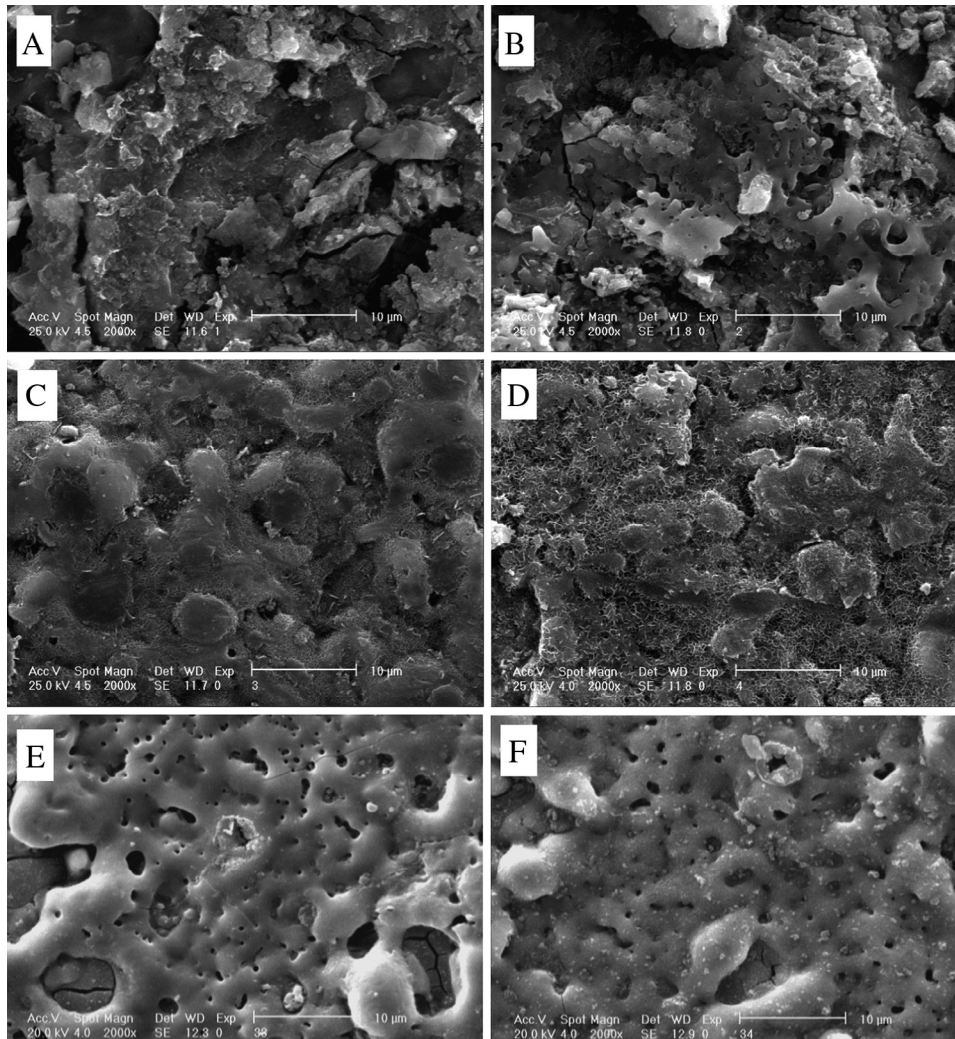| Sample code	R_a (µm)
S-0-1	1.89
S-0-2	1.63
S-5-1	1.15
S-5-2	0.933
R-0-0	0.842
R-5-0	0.733

Fig. 2. SEM images of the free coating surfaces, showing (A) S-0-1, (B) S-0-2, (C) S-5-1, (D) S-5-2, (E) R-0-0, and (F) R-5-0.

that the presence of nanoparticle in electrolyte with potassium stearate created new phases on the surface of the coating. The structure of this phase is similar to the nanosheets deposited from the stearate chain which was previously reported in ethanolic stearic acid solution by Huang et al. [11]. These sediments have low surface energies, and also their large surface and roughness property can lead to increase in contact angle from hydrophilic to hydrophobic, and this will be discussed in the contact angle results.

Fig. 4 illustrates the AFM images of the sheet-shaped structure observed in Fig. 3 on the S-5-1 coating's surface. The roughness profile has been plotted for the line specified in Fig. 4 and shown in Fig. 5. The width of a sheet in the roughness profile is approximately 410 nm which seems larger than the observed size in Fig. 3 due to the laminated deposition of several layers.

Fig. 6A shows the photograph of a cross-section of nanocomposite coating related to the S-5-1 sample taken by a transmission electron microscope. A matrix of amorphous magnesium oxide and dispersed silicon nitride particles can be observed in Fig. 6A.

Fig. 6B shows the photograph of alcohol dispersed hydrophobic nanoparticle related to the S-5-1 sample taken by a transmission electron microscope. Agglomerated chains of stearate assembled on nanoparticle and made it hydrophobic. Hydrophobic nanoparticles are insoluble in water and deposited on coating surface. Other researchers [12] used fluorine based functional nanoparticle to increase hydrophobicity so it is possible that stearate assembled silicon nitride has increased contact angle.

The curves of the Wilhelmy plate force versus immersion depth are shown in Fig. 7. Results of static contact angle, contact angle hysteresis, and surface tension are calculated from Fig. 7 which is also reported in Table 3. The result of Wilhelmy plate test showed that immersion (advancing contact angle) data have more negative force than emersion data (receding angle angle) and this indicates that the coating was wetted [13]. The immersion data of Wilhelmy plate is jagged but emersion data are smooth, which is compatible with the results obtained by other researchers [14]. The additives had no significant effect on the receding dynamic contact angle which confirms the results obtained by other researchers [15] on the effect of composition on wettability. The hysteresis of the Cassie–Baxter model in Wilhelmy plate was less than 10° [16], therefore the Wenzel model was dominant on this coating which
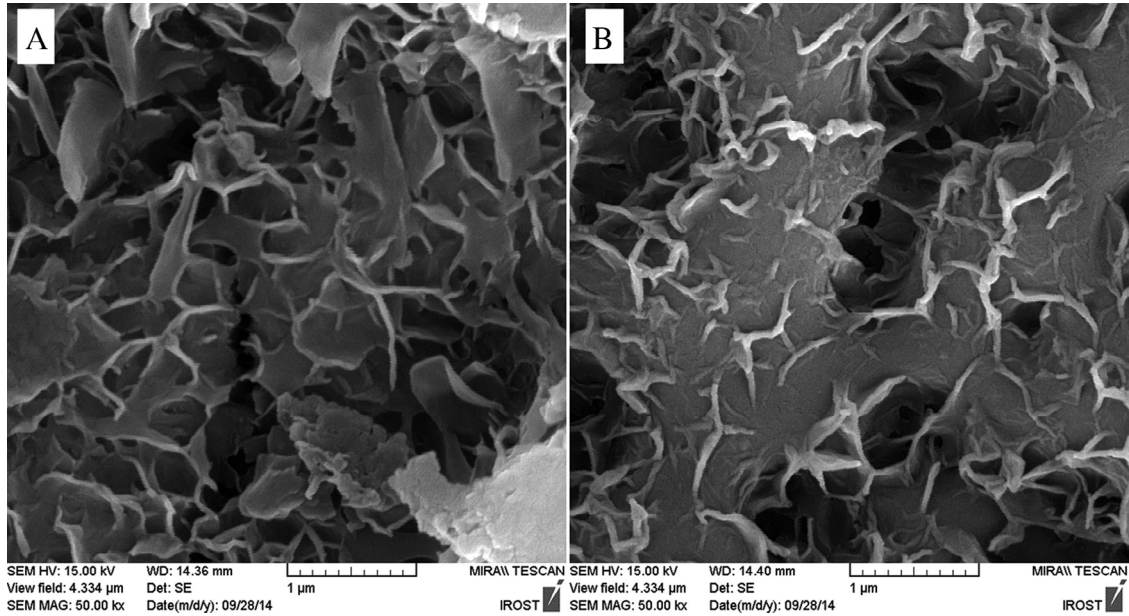
Fig. 3. SEM image of surface of nanocomposite samples including (A) S-5-1 and (B) S-5-2.

was realized by an extension of the hysteresis contact angle. Extension of hysteresis contact angle by potassium stearate additive increased the work of adhesion [17] and made the coating sticky.

At the micro-scale, traditional coatings (S-0-1 and S-0-2) showed more roughness properties as compared to the nanocomposite coatings (Table 2); however, nanocomposite coatings (S-5-1 and S-5-2) and specimens showed more
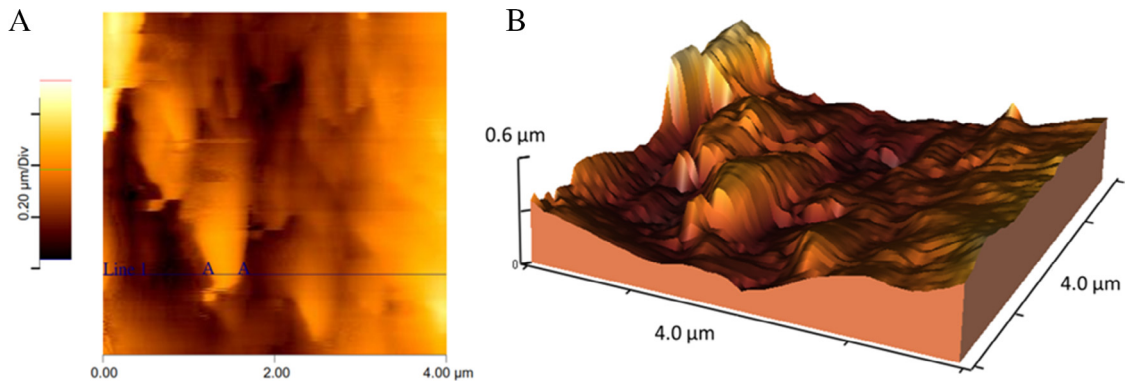

Fig. 4. AFM images of the surface of S-5-1 sample (A) two-dimensional, (B) three-dimensional.
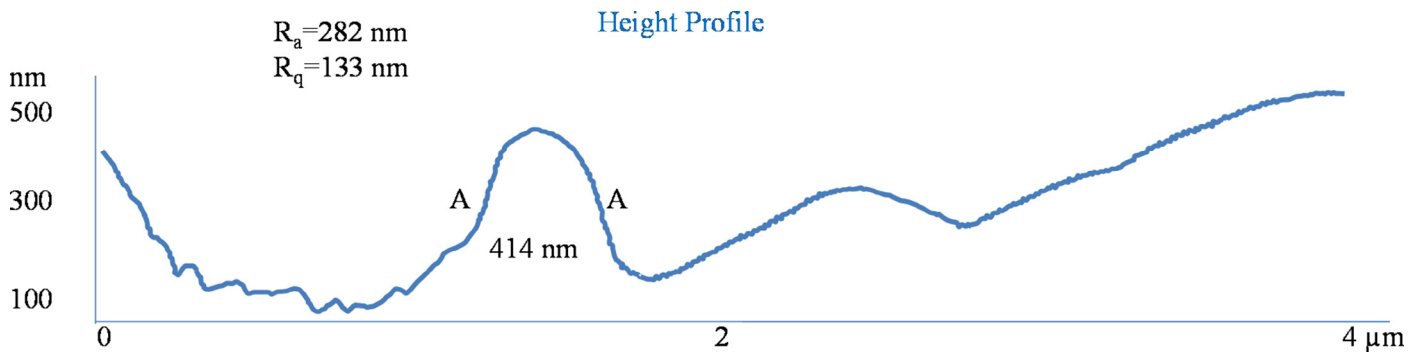

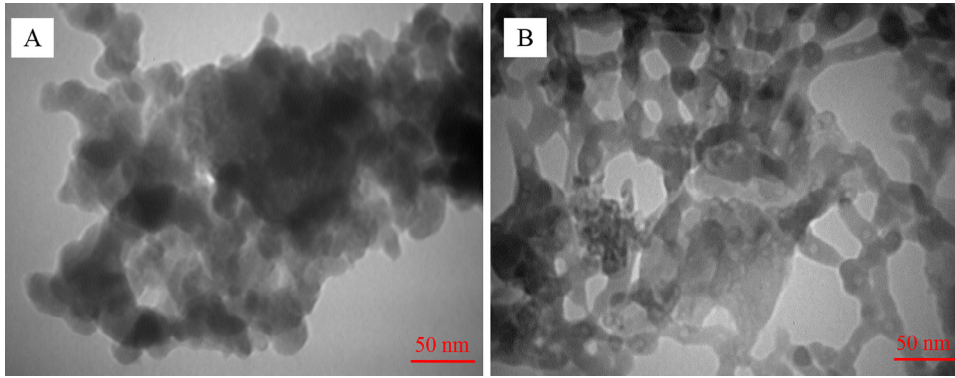Fig. 5. Roughness profile of the line specified in figure 5.

Fig. 6. TEM image from scratched debris of sample S-5-1 (A) water dispersed coating particles, (B) alcohol dispersed coating particles.

roughness at the nano-scale due to the deposition of stearate chains (Fig. 3). All traditional and nanocomposite specimens showed roughness criteria lower than 2 μm (Table 2). The minimum roughness criterion to attain Cassie and Baxter model is reported as 8 μm [18]; consequently, the PEO coating have no sufficient roughness to attain the Cassie and Baxter model.

Two mechanisms exist for surface tension modification. The first mechanism is Self-Assembled Monolayer which occurs by smooth surface [19,20] and the second mechanism is the deposition of a low energy flower-like structure shape [21] which is accompanied by increase in roughness. Consequently, it can be concluded that stearate nanosheets possess both prerequisites for achieving hydrophobicity, including low surface energy effect and roughness effect. The contact angle of the S-0-1 sample is 131 degrees, according to Wenzel models, and the contact angel is affected by surface roughness
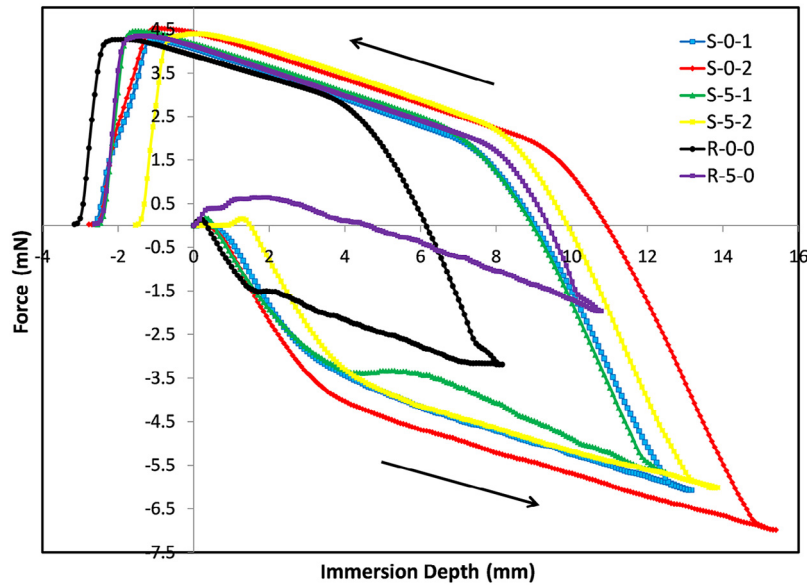

Fig. 7. Curves of Wilhelmy plate force vs immersion depth for the specimens.

Table 3
Wettability results of the coatings.

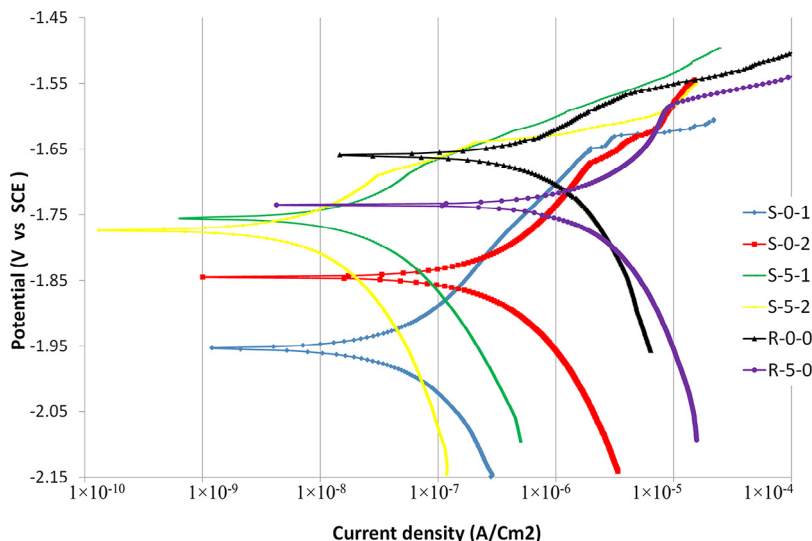| Sample code	Static contact angle (degree)	Advancing contact angle (degree)	Receding contact angle (degree)	Hysteresis contact angle (degree)	Surface tension (N/m)
S-0-1	131	107	60	47	16
S-0-2	125	110	63	47	14
S-5-1	91	104	62	42	18
S-5-2	110	106	60	46	16
R-0-0	49	96	64	32	24
R-5-0	44	82	63	20	35

Fig. 8. Curves of polarization test results for the coatings.

based on the following equation in which "r" is the roughness factor [22]:

$$Cos\,\Theta_{rough} = r\,Cos\,\Theta_{flat} \qquad (1)$$

In the case of sample S-0-1, the roughness factor of the surface is nearly 2 for the Wenzel equation because the lowest surface energy [8] is attributed to the 111° contact angle and S-0-1 sample just could increase the contact angle by surface roughness. Advancing and receding contact angles are used in Chibowski formula [23] to calculate the surface tension. Regarding the Wenzel model wettability, surface tension value obtained from the thermodynamic equations was calculated for a roughness coefficient equal to 2 using the Chibowski formula reported in Table 3.

Comparing the static contact angles of S-0-1 and R-0-0 samples implies that the addition of potassium stearate to the electrolyte of traditional coatings increased the static contact angle from 49° to 131° and transited the specimen from hydrophilic to hydrophobic coating. Potassium stearate with deposits of organic stearate chains on the surface decreased the surface tension for traditional coatings from 24 to 16 N/m.

The static contact angle is inversely correlated with an increase in the concentration of potassium stearate in the electrolyte of traditional coatings and finally reached 125° (by comparing S-0-1 and S-0-2 angles) which confirmed all other results [20].

The addition of potassium stearate in the electrolyte of nanocomposite coatings increased the static contact angle from 44° to 91°. The static contact angle was found to be directly correlated with the concentration of potassium stearate on the nanocomposite coating and reached 110° and potassium stearate decreased the surface tension by 54%. The different effect of additive concentration on traditional and nanocomposite coatings can be explained by the synergistic effect of potassium stearate and nanoparticle. Assembling of fatty acid on ceramic powder [24] caused an increase in the hydrophobicity. It seems

that the use of additive and nanoparticle together increased the deposition of hydrophobic nanoparticles on the coating and this is responsible for the increase in contact angle.

The highest static contact angle is related to the S-0-1 sample which provides a sufficient reduction in the surface tension, in order to form a hydrophobic coating. However, the PEO process did not provide the required roughness of superhydrophobicity because roughness was not high enough at the micro-scale to attain the Cassie and Baxter model and decrease contact angle hysteresis.

Roughness criterion to attain more hydrophobicity [18] was also reported for Wilhelmy plate [25] and it indicated that rougher PEO coating was needed to attain the Cassie model and also to decrease the Wilhelmy hysteresis extension.

Fig. 8 and Table 4 show polarization curves results for the coatings. Comparing the corrosion behaviour of S-0-1 and R-0-0 implied that potassium stearate possessed a decreased corrosion rate for traditional specimens by fifteen-fold and a changed corrosion potential from 0.3 V to more active values. In spite of the fact that the additive is more active than the substrate, it decreased the corrosion rate by increasing the hydrophobicity, and this confirmed all other results [20].

By comparing the corrosion behaviour of S-0-2 and R-0-0 samples, it appears that the reduction of corrosion rate and more active corrosion potential for ordinary PEO coating is inversely correlated with the concentration of the additive. An

Table 4
Results obtained from polarization curves.

Sample code	i_{cor} (A/cm^2)	E_{cor} (V)
S-0-1	6.0E-08	−1.94
S-0-2	3.5E-07	−1.83
S-5-1	2.0E-08	−1.76
S-5-2	1.0E-08	−1.78
R-0-0	9.0E-07	−1.65
R-5-0	2.5E-06	−1.75

S.S. Farhadi et al./Journal of Magnesium and Alloys 5 (2017) 210–216

increase in the concentration of the additive reduced the corrosion rate by 2.5-fold because the concentration of the additive had a reverse correlation as a result of hydrophobicity.

Potassium stearate showed 125-fold decrease in the corrosion rate of the nanocomposite coating (by comparing S-5-1 and R-5-0 samples). An increase in the concentration of potassium stearate for nanocomposite coatings decreased the corrosion rate by 250-fold because of the more static contact angle.

For samples without additive (by comparing R-0-0 and R-5-0 samples), nanoparticle increased the corrosion rate by nearly threefold. The effect of the presence of nanoparticle with additive is opposed to that of coatings without additive, because of the synergistic effect of the nanoparticle and additive on hydrophobicity.

Addition of potassium stearate shifted corrosion potentials to the active values and decreased the corrosion rate which confirmed the results obtained by other researchers in coating of myristic acid on copper substrate [26], but nobler magnesium coating was just reported on the super-hydrophobic surface [6,27]. PEO is effective method by which the properties of substrate can be improved [28–30], especially for Mg alloys [31]. In this study, it can be concluded that by applying PEO treatment, hydrophobic coatings can be obtained.

4. Conclusions

1 The addition of potassium stearate increased contact angle by up to 131° and decreased the surface tension of coatings up to 54%.
2 Potassium stearate decreased corrosion rate of coating by up to 250-fold.
3 Potassium stearate provides the required reduction in surface tension for transformation into a superhydrophobic coating; however, the roughness of the plasma electrolytic oxidation process did not provide the necessary roughness to form a superhydrophobic coating.
4 The use of additive and nanoparticle together increased the deposition of hydrophobic nanoparticles (self-assembled layer of fatty acid on ceramic powder) on the coating and this is responsible for the increase in contact angle.

References

[1] J. Guo, L. Wang, S. Wang, J. Liang, Q. Xue, F. Yan, J. Mater. Sci. 44 (8) (2009) 1998–2006.
[2] Y. Fan, Z. Chen, J. Liang, Y. Wang, H. Chen, Surf. Coat. Technol. 244 (2014) 1–8.
[3] R.M. Wu, S.Q. Liang, H. Chen, A.Q. Pan, H.Y. Jiang, J. Deng, et al., Appl. Mech. Mater. 200 (2012) 190–193.
[4] Y. Yin, T. Liu, S. Chen, T. Liu, S. Cheng, Appl. Surf. Sci. 255 (5) (2008) 2978–2984.
[5] S.V. Gnedenkov, V.S. Egorkin, S.L. Sinebryukhov, I.E. Vyaliy, A.S. Pashinin, A.M. Emelyanenko, et al., Surf. Coat. Technol. 232 (2013) 240–246.
[6] S. Gnedenkov, S. Sinebryukhov, V. Egorkin, D. Mashtalyar, A. Emelyanenko, L. Boinovich, J. Taiwan Inst. Chem. Eng. 45 (6) (2014) 3075–3080.
[7] S. Wang, X. Guo, Y. Xie, L. Liu, H. Yang, R. Zhu, et al., Surf. Coat. Technol. 213 (2012) 192–201.
[8] M.A. Raza, E.S. Kooij, A. van Silfhout, H.J. Zandvliet, B. Poelsema, J. Colloid Interface Sci. 385 (1) (2012) 73–80.
[9] L.M. Lander, L.M. Siewierski, W.J. Brittain, E.A. Vogler, Langmuir 9 (8) (1993) 2237–2239.
[10] A. Seyfoori, S. Mirdamadi, Z.S. Seyedraoufi, A. Khavandi, M. Aliofkhazraei, Mater. Chem. Phys. 142 (1) (2013) 87–94.
[11] Y. Huang, D. Sarkar, X. Chen, Mater. Lett. 64 (24) (2010) 2722–2724.
[12] J.-D. Brassard, D. Sarkar, J. Perron, Appl. Sci. 2 (2) (2012) 453–464.
[13] R.L. Bendure, J. Colloid Interface Sci. 42 (1) (1973) 137–144.
[14] T.H. Muster, A.K. Neufeld, I.S. Cole, Corros. Sci. 46 (9) (2004) 2337–2354.
[15] J. Chen, G. Luo, W. Cao, J. Colloid Interface Sci. 238 (1) (2001) 62–69.
[16] H. Chen, F. Zhang, T. Chen, S. Xu, D.G. Evans, X. Duan, Chem. Eng. Sci. 64 (12) (2009) 2957–2962.
[17] S.J. Pogorzelski, Z. Berezowski, P. Rochowski, J. Szurkowski, Appl. Surf. Sci. 258 (8) (2012) 3652–3658.
[18] W. Xu, J. Song, J. Sun, Y. Lu, Z. Yu, ACS Appl. Mater. Interfaces 3 (11) (2011) 4404–4414.
[19] C.Y. Chen, L.H. Chen, Y.L. Lee, J. Chin. Inst. Chem. Eng. 32 (5) (2001) 461–468.
[20] Z. ajdari, H.O. Ćurković, V. Čadež, S. Šegota, J. Electrochem. Soc. 163 (5) (2016) C145–C155.
[21] J.-H. Li, Q. Liu, Y.-L. Wang, R.-R. Chen, K. Takahashi, R.-M. Li, et al., J. Electrochem. Soc. 163 (5) (2016) C213–C220.
[22] Y. Yan, N. Gao, W. Barthlott, Adv. Colloid Interface Sci. 169 (2) (2011) 80–105.
[23] E. Chibowski, Adv. Colloid Interface Sci. 103 (2) (2003) 149–172.
[24] Y. Wang, B. Li, C. Xu, Superlattices Microstruct. 51 (1) (2012) 128–134.
[25] K. Abe, H. Takiguchi, K. Tamada, Langmuir 16 (5) (2000) 2394–2397.
[26] I. Milošev, T. Kosec, M. Bele, J. Appl. Electrochem. 40 (7) (2010) 1317–1323.
[27] B. Yin, L. Fang, J. Hu, A.-Q. Tang, W.-H. Wei, J. He, Appl. Surf. Sci. 257 (5) (2010) 1666–1671.
[28] H. Sharifi, M. Aliofkhazraei, G.B. Darband, A.S. Rouhaghdam, Tribol. Int. 102 (2016) 463–471.
[29] M. Asgari, M. Aliofkhazraei, G.B. Darband, A.S. Rouhaghdam, Surf. Coat. Tech. 309 (2017) 124–135.
[30] M. Aliofkhazraei, R.S. Gharabagh, M. Teimouri, M. Ahmadzadeh, G.B. Darband, H. Hasannejad, J. Alloys Compd. 685 (2016) 376–383.
[31] G. Barati Darband, M. Aliofkhazraei, P. Hamghalam, N. Valizade, J. Magnes. Alloys 5 (2017) 74–132.